Bistability in active circuits: Application of a novel Fokker–Planck approach

by Peter Hänggi
Peter Jung

The problem of metastability in electronic circuits with negative differential resistance, originally pioneered by Landauer in 1962, is reconsidered from the viewpoint of a Fokker–Planck modeling for nonlinear shot noise (master equation). A novel Fokker–Planck approximation scheme is presented that describes correctly the deterministic flow and the long-time dynamics of the master equation. It is demonstrated that the conventional scheme of a truncated Kramers–Moyal expansion at the second order overestimates the transition rates in leading exponential order. In order to obtain the correct relative stability, the novel scheme uses a diffusion coefficient which incorporates information about global nonlinear fluctuations characterized by the whole set of all higher-order Kramers–Moyal transport coefficients.

1. Introduction

The study of dissipative elements which are able to hold information, or, more generally, the role of relative stability in systems which continuously dissipate energy, was pioneered and influenced by Rolf Landauer. The school around Stratonovich [1] (i.e., Stratonovich and coworkers such as V. I. Tikhonov and P. I. Kuznetsov) and independently Landauer [2] were the first to describe first- or second-order-type transitions in driven nonequilibrium systems. In his paper entitled "Fluctuations in Bistable Tunnel Diode Circuits" [2], Landauer discusses distribution functions and jump rates of metastable states far from thermal equilibrium. The results of this paper clearly demonstrate that questions about relative stability in driven systems far from equilibrium cannot be answered by an appeal to the deterministic flow or local stability criteria. The random force in this bistable system which drives the system away from locally stable states depends upon the state variable itself; thus the noise variation along the whole escape path matters in evaluating the relative stability of a metastable state.

The problem of metastability in stationary nonequilibrium systems determines the physical behavior in a variety of systems including optical bistability [3], chemical systems [4], and biology [5]. In this work we take a new look at the dynamics of Landauer's bistable tunnel diode model (see also [6]). We focus on a Fokker–Planck approximation to the exact master equation dynamics, a problem which has been tackled previously. van Kampen [7] has introduced the system size expansion, which results in a local description around the deterministic law of the master equation dynamics in terms of a "linear" Fokker–Planck equation [7]

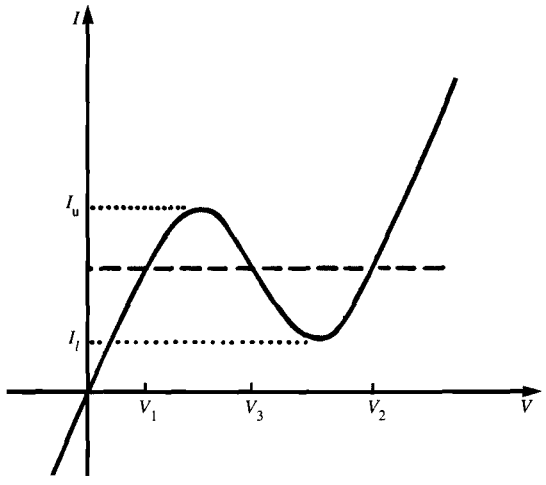

Figure 1

Static current–voltage characteristic $I(V)$ of a tunnel diode. For driving currents I_{dr} (dashed line) between I_l and I_u there exist two stable stationary states at V_1 and V_2, and one unstable state at V_3.

with a linear drift and a state-independent diffusion coefficient. Thus, this approximation cannot describe large nonlinear fluctuations and global features such as the relative stability between neighboring metastable states. A global Fokker–Planck approximation can be obtained by truncating the Kramers–Moyal expansion of the master equation after the second term [2, 4]. This is, in fact, the most widely used approximation scheme. However, as Landauer had already noted in 1962 [2], the stationary dynamics of this conventional approximation scheme does not reproduce the correct state-continuous version of the exact master equation solution. A novel Fokker–Planck approximation to a master equation dynamics obeying detailed balance which supersedes the conventional scheme has been put forward recently [8–10]. This latter method is based on nonlinear transport theory for master equations [8, 9]; in particular, the Fokker–Planck coefficients become state-dependent functions, and, more importantly, they encompass information about all higher-order Kramers–Moyal moments.

The paper is organized as follows. In Section 2 the current–voltage characteristic of a tunnel diode is discussed, using phenomenological laws for the elementary current components. Taking into account the shot noise due to the quantization of the charge, we arrive in Section 3 at a birth–death master equation for the charge on the diode capacitance. The exact stationary distribution and the asymptotic form for large system sizes are also presented in this section. Moreover, we introduce the Kramers–Moyal expansion and cast the deterministic law into a generalized Onsager form. In Section 4 we present the conventional Fokker–Planck approximation scheme. We compare the stationary probability obtained from the master equation with that of the truncated Kramers–Moyal Fokker–Planck equation. In Section 5 we apply the novel Fokker–Planck approximation scheme and evaluate the transition rates. The results of the different Fokker–Planck approximations are compared with those of the master equation.

2. Current–voltage characteristic of a tunnel diode

Usually electrical circuits have a current–voltage characteristic with positive slope, corresponding to a positive differential resistance. Some highly doped semiconductor devices, however, have regions in the characteristic with a negative differential resistance. One of these semiconductor devices is the well-known tunnel diode. The negative differential resistance of the tunnel diode device is due to a tunneling current from the valence band of the n-doped region to the conducting band of the p-doped region. **Figure 1** shows a typical current–voltage characteristic for a tunnel diode, driven by a current source I_{dr}. For $I_u > I > I_l$ there are two stable voltages V_1 and V_2. The voltage V_3 is unstable. For $I \to I_{u-}$ and $I \to I_{l+}$ the stable states V_1 and V_2, respectively, lose their stability, and switching occurs to the other stable state. The tunnel diode is a driven system which exhibits a discontinuous nonequilibrium phase transition between a low-voltage state V_1 and a high-voltage state V_2. The current through the tunnel diode is broken up into two terms

$$I = I_Z + I_E, \tag{1}$$

with the "Zener" current I_Z being due to valence electrons tunneling into the conduction band. The "Esaki" current I_E is due to conduction electrons tunneling into the valence band plus the thermal diffusion current of electrons. A particular model for these currents is [11]

$$I_Z(V) = -I_0 \exp(-\bar{J}V),$$

$$I_E(V) = I_0 \exp[-\bar{K}V(V - \bar{V}_0)] + S_0[\exp(\bar{T}V) - 1], \tag{2}$$

where the parameters I_0, $\bar{J}$, $\bar{K}$, $\bar{T}$, S_0, and $\bar{V}_0$ are parameters to fit the measured current–voltage characteristic. The Zener current is charging the diode capacitance and therefore has the opposite sign from the discharging Esaki current. To end up with a description which does not depend on the system size Ω (= area of the diode p–n interface), we introduce the intensive quantities

$$n = V\frac{C}{e\Omega}$$

and

$$j = \frac{I}{\Omega}. \tag{3}$$

Here n is the electron excess density per unit charge e and j is the current density. The current–voltage characteristic now reads

$$j(n) = -j_0\exp(-Jn) + j_0\exp[-Kn(n - n_0)] + s_0[\exp(Tn) - 1], \quad (4)$$

with new parameters j_0, J, K, s_0, T, and n_0.

3. Tunnel diode with noise: Master equation

We take the discrete nature of the charge into account and describe the state of the tunnel diode system driven by a constant current source I_{dr} by the number N of excess unit charges on the diode capacitance C. The voltage across the diode is then given by $V = eN/C$. The capacitance is charged by the sum of the driving current I_{dr} and the Zener current I_Z, and discharged by the Esaki current I_E. We assume that all contributions consist of uncorrelated transfers of single electrons. Then we obtain a birth-and-death process described by the master equation [2],

$$\dot{P}(N, t) = W^+(N - 1)P(N - 1, t) + W^-(N + 1)P(N + 1, t) - [W^+(N) + W^-(N)]P(N, t) \qquad N = 0, \pm1, \pm2, \cdots, \quad (5)$$

where $W^+(N)$ is the transition rate from the state N to $N + 1$, and $W^-(N)$ is the transition rate from state N to $N - 1$, i.e.,

$$W^+(N) = \frac{1}{e}[I_{dr}(N) - I_Z(N)],$$

$$W^-(N) = \frac{1}{e}I_e(N). \quad (6)$$

Because the master equation represents a one-dimensional stochastic process with natural boundaries, detailed balance is valid, i.e.,

$$W^-(N + 1)P_{St}(N + 1) = W^+(N)P_{St}(N) \quad (7)$$

The stationary distribution P_{St} is thus given by

$$P_{St}(N) = \frac{1}{Z}\exp[-\phi(N)] \quad (8)$$

(where Z denotes the normalization), with the potential

$$\phi(N) = -\sum_{K=N_0}^{N-1}\ln\frac{W^+(K)}{W^-(K + 1)}. \quad (9)$$

Next we want to derive a continuous description of the above discrete process. With the scaling relation

$$W^{\pm}(N) = \Omega\gamma^{\pm}(n), \quad (10)$$

the intensive density n [Equation (3)] and its probability $p_t(n)$ are given by

$$n = \frac{N}{\Omega}, \qquad p_t(n) = \Omega P_t(N). \quad (11)$$

The Kramers–Moyal expansion of the master equation (5) thus reads

$$\dot{p}_t(n) = \sum_{\nu=1}^{\infty}\frac{1}{\nu!}\frac{1}{\Omega^{\nu-1}}\left(-\frac{\partial}{\partial n}\right)^{\nu}A_\nu(n)p_t(n). \quad (12)$$

The Kramers–Moyal moments $A_\nu(n)$ are simply given by

$$A_\nu(n) = \gamma^+(n) + (-1)^\nu\gamma^-(n), \quad (13)$$

and the transition rates $\gamma^+(n)$ and $\gamma^-(n)$ are connected to the current densities

$$\gamma^+(n) = j_{dr} + j_0\exp(-Jn),$$
$$\gamma^-(n) = j_0\exp[-Kn(n - n_0)] + s_0[\exp(Tn) - 1]. \quad (14)$$

To evaluate the stationary distribution function for the density n, we insert Equations (10) and (11) into the exact stationary distribution [Equations (8) and (9)] and replace the summation over the discrete variable N with an integration over the density n. Including the "start" and "end" points of the summation N_0 and $N - 1$ symmetrically, i.e., $N_0 \to N_0 - \frac{1}{2}$; $N - 1 \to N - \frac{1}{2}$, one obtains the result

$$p_{St}(n) = \frac{1}{Z}\exp\left\{-\Omega\left[\phi_0(n) + \frac{1}{\Omega}\phi_1(n)\right]\right\} + O(\Omega^{-1}). \quad (15)$$

The leading-order potential $\phi_0(n)$ reads

$$\phi_0(n) = -\int_{n_0}^{n}\ln\frac{\gamma^+(y)}{\gamma^-(y)}\,dy, \quad (16)$$

and the first-order correction $\phi_1(n)$ is

$$\phi_1(n) = -\frac{1}{2}\ln\left[\frac{\gamma^+(n_0)\gamma^-(n_0)}{\gamma^+(n)\gamma^-(n)}\right]. \quad (17)$$

Detailed balance in Equation (7) now implies the following relationship between the drift and higher-order moments [8]:

$$A_1(n) = -\frac{1}{2}p_{St}(n)^{-1}\sum_{\nu=1}^{\infty}\frac{1}{\nu!}\frac{1}{\Omega^\nu}\left(-\frac{\partial}{\partial n}\right)^{\nu}A_{\nu+1}(n)p_{St}(n). \quad (18)$$

Inserting Equation (15) into (18), one finds in the limit $\Omega \to \infty$ for the deterministic flow the *Onsager form*, i.e.,

$$\dot{n} = A_1(n) = -L(n)\chi_0(n), \quad (19)$$

with the generalized thermodynamic force

$$\chi_0(n) = \frac{\partial\phi_0(n)}{\partial n} = \ln\gamma^-(n) - \ln\gamma^+(n). \quad (20)$$

The positive transport coefficient $L(n)$ is given by

$$L(n) = \frac{1}{2}\sum_{\nu=0}^{\infty}\frac{1}{(\nu + 1)!}A_{\nu+2}(n)[\chi_0(n)]^\nu = \frac{\gamma^+(n) - \gamma^-(n)}{\ln\gamma^+(n) - \ln\gamma^-(n)} > 0. \quad (21)$$

To guarantee the stability of the deterministic flow

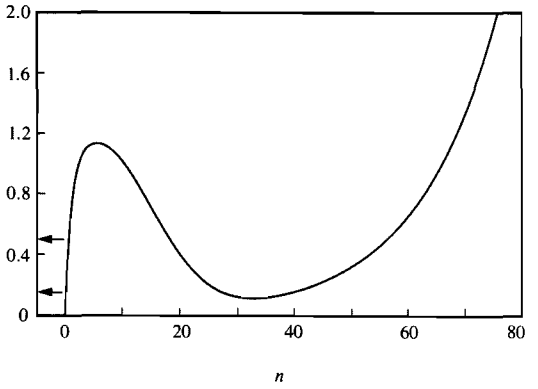

Figure 2

The current density–electron excess density characteristic of a tunnel diode (4). The parameter values used are $j_0 = 1, K = 0.005, J = 1$, $s_0 = 0.01$, $n_0 = 10$, and $T = 0.07$. The two driving currents used in the explicit calculations are indicated by arrows at $j_{dr} = 0.15$, $j_{dr} = 0.5$.

[Equation (19)] we note that $\phi_0(n)$ is a Liapunov function, i.e., with Equation (19)

$$\frac{d}{dt}\phi_0 = \chi_0(n)\frac{dn}{dt} = -\chi_0(n)L(n)\chi_0(n) < 0. \tag{22}$$

The function $\phi_0(n)$ is bounded from below because the distribution function $p_{St}(n)$ [Equation (15)] is normalized. In higher-dimensional systems the existence of such a Liapunov function can also be shown [8]; however, the corresponding derivation for the semipositive transport matrix $\mathbf{L}(n)$ is nontrivial [8]. The transport equation (19) is the starting point for a novel Fokker–Planck approximation originally put forward in References [9, 10]. First, however, let us consider the conventional Fokker–Planck modeling. Clearly, such a Fokker–Planck modeling (or approximation) is preferred because it is analytically more tractable than the master equation (infinite-order partial differential equation).

4. Conventional Fokker–Planck model

For large system size Ω the discreteness of the one-step process is of minor importance, and we might approximate the discrete process by a state-continuous process. The conventional scheme to approximate the discrete process by a Fokker–Planck equation is to truncate the Kramers–Moyal expansion [Equation (12)] after the second term, i.e.,

$$\dot{p}_t(n) = -\frac{\partial}{\partial n}A_1(n)p_t(n) + \frac{1}{2\Omega}\frac{\partial^2}{\partial n^2}A_2(n)p_t(n), \tag{23}$$

where

$$A_1(n) = \gamma^+(n) - \gamma^-(n), \qquad A_2(n) = \gamma^+(n) + \gamma^-(n). \tag{24}$$

The stationary probability is readily found by quadratures

$$p_{St}(n) = \frac{1}{Z}\frac{1}{A_2(n)}\exp[-\Omega\psi_0(n)], \tag{25}$$

with the Fokker–Planck potential

$$\psi_0(n) = -2\int_{n_0}^{n}\frac{\gamma^+(y) - \gamma^-(y)}{\gamma^+(y) + \gamma^-(y)}\,dy. \tag{26}$$

Here one notices that the Fokker–Planck potential $\psi_0(n)$ [Equation (26)] *does not agree* with the asymptotic potential $\phi_0(n)$ [Equation (16)] *even in the leading order.* However, the positions of the extrema, as well as the curvature at the extrema, coincide in both potentials. The difference in the generalized thermodynamic force is given by

$$\frac{\partial\phi_0(n)}{\partial n} - \frac{\partial\psi_0(n)}{\partial n} = -\ln\frac{\gamma^+(n)}{\gamma^-(n)} + 2\,\frac{\gamma^+(n) - \gamma^-(n)}{\gamma^+(n) + \gamma^-(n)}. \tag{27}$$

• *Comparison of the potentials*

In **Figure 2** the characteristic of the tunnel diode [Equation (4)] is depicted for the parameter values $j_0 = 1$, $K = 0.005$, $J = 1$, $s_0 = 0.01$, $n_0 = 10$, and $T = 0.07$. This current–voltage shape agrees with experimental measured tunnel-diode characteristics [11]. In **Figures 3(a)** and **3(b)** the corresponding asymptotic potential $\phi_0(n)$ [Equation (16)] of the master equation is compared to the potential $\psi_0(n)$ [Equation (26)] of the Kramers–Moyal Fokker–Planck equation for the driving current $j_{dr} = 0.15$ (a), and for $j_{dr} = 0.5$ (b). The potentials both have minima at the operating point (i.e., the intersection of the current–voltage characteristic and the driving current j_{dr} = const.) of the diode that corresponds to a positive differential resistance. The relative maximum of the potential corresponds to the unstable state at $V = V_3$. A simple shift of the whole potential is not relevant, as it can always be compensated in terms of a renormalization for the probability. Differences in *shape*, however, impact the barrier heights. For example, the barrier height for forward transitions of the Fokker–Planck modeling differs by $\approx 17\%$ for $j_{dr} = 0.15$, and differs by $\approx 2\%$ for $j_{dr} = 0.5$, respectively, relative to the master equation value. In **Figure 3(c)** we compare the thermodynamic force of the master equation process with the force due to the conventional Fokker–Planck approximation at the driving current density $j_{dr} = 0.5$.

5. Novel Fokker–Planck approximation

The conventional Fokker–Planck approximation does not coincide with the continuum limit of Equations (8) and (9) of the stationary probability of the master equation, and this difference does not vanish in the limit $\Omega \to \infty$. The correct stationary probability is also influenced by the higher-order Kramers–Moyal moments [Equation (13)] which thus must be accounted for. We observe that for any Fokker–Planck

modeling having the correct asymptotic stationary probability [Equation (15)], the drift and diffusion coefficients must be related by

$$\tilde{A}_1(n) = -\tfrac{1}{2}\tilde{A}_2(n)\chi_0(n) + O(\Omega^{-1}). \tag{28}$$

Since the deterministic law is recovered only if we use [see Equation (19)]

$$\tilde{A}_1(n) = -L(n)\chi_0(n) + O(\Omega^{-1}), \tag{29}$$

it follows that

$$\tilde{A}_2(n) = 2L(n) + O(\Omega^{-1}). \tag{30}$$

Hence, apart from terms of higher order in Ω^{-1}, the diffusion coefficient

$$\tilde{A}_2(n) \equiv 2L(n) \tag{31}$$

is fixed by the stationary probability [Equation (15)] and the Onsager transport law [Equation (19)]. On the basis of the thermodynamic potential for the stationary probability in Equation (16), we obtain, in terms of the first two leading contributions $\phi_0(n)$ and $\phi_1(n)$ in Equations (15) and (31), the novel Fokker–Planck approximation [9, 10]

$$\dot{p}_t(n) = \frac{\partial}{\partial n} L(n)\left[\chi_0(n) + \frac{1}{\Omega}\chi_1(n) + \frac{1}{\Omega}\frac{\partial}{\partial n}\right] p_t(n) \tag{32a}$$

with

$$\chi_0(n) = \frac{\partial\phi_0(n)}{\partial n}, \qquad \chi_1(n) = \frac{\partial\phi_1(n)}{\partial n}. \tag{32b}$$

If we compare Equations (32) with the conventional Fokker–Planck approximation in Equations (23) and (24), we note that the new Fokker–Planck coefficients are related to the conventional coefficients by

$$\tilde{A}_1(n) = A_1(n) + \frac{1}{\Omega}\left[\frac{\partial L(n)}{\partial n} - L(n)\chi_1(n)\right] \tag{33}$$

and

$$\tilde{A}_2(n) = A_2(n) + \sum_{r=1}^{\infty}\frac{1}{(r+1)!}A_{r+2}(n)[\chi_0(n)]^r. \tag{34}$$

In particular, the state-dependent diffusion in Equation (34) explicitly involves the higher-order Kramers–Moyal transport coefficients $A_\nu(n)$, $n > 2$. The difference $\tilde{A}_2(n) - A_2(n)$, being proportional to powers of the thermodynamic force χ_0, is plotted in **Figure 4**. Interestingly enough, for *any birth-and-death process* this difference of state-dependent diffusion coefficients is *always negative semidefinite*. The difference equals zero precisely at the deterministic steady states only. Thus the conventional Fokker–Planck approximation everywhere overestimates the actual physical noise strength $D(n)$; i.e., $\langle\xi(n, t)\xi(n, s)\rangle \equiv D(n)\delta(t - s)$. Using Equations (34) and (13), this result follows due to the inequality

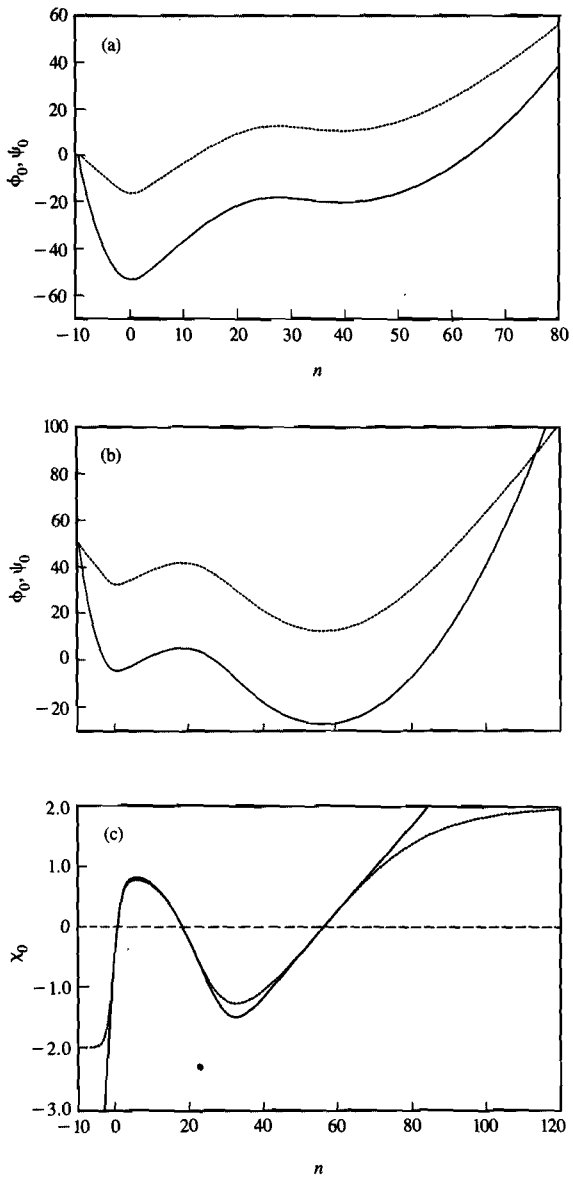

Figure 3

(a) Comparison between the two thermodynamic potentials for a driving current density $j_{dr} = 0.15$. Solid line: master equation result (16); broken line: Kramers–Moyal Fokker–Planck approximation (26). (b) Comparison between the two thermodynamic potentials for a driving current density $j_{dr} = 0.5$, lying approximately halfway between j_l and j_u. Solid line: master equation result (16); broken line: conventional Fokker–Planck approximation (26). (c) The thermodynamic force $\chi_0(n) = \partial\phi_0/\partial n$, (20), for the master equation dynamics (solid line) compared with the thermodynamic force $\partial\phi_0/\partial n$, (27), of the corresponding Kramers–Moyal Fokker–Planck approximation (broken line). The driving current density is $j_{dr} = 0.5$. Note that at the steady states the two forces agree in value [i.e., $\chi_0(n_1) = \chi_0(n_2) = \chi_0(n_3) = 0$] and slope; thus the curvatures of the two potentials agree at the extrema points.

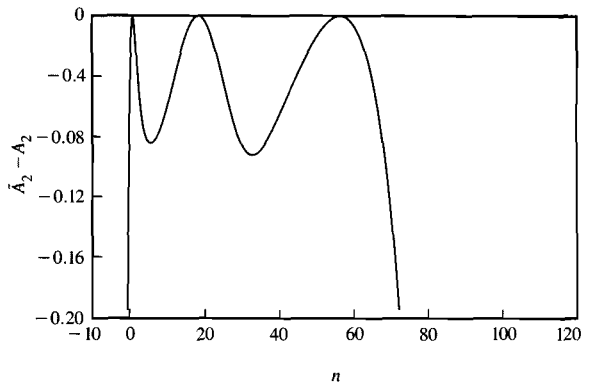

Figure 4

The difference between the state-dependent diffusion coefficients $\tilde{A}_2(n) - A_2(n)$, (34), of the two Fokker–Planck approximations. The driving current density is $j_{dr} = 0.5$; this implies for the diffusion coefficient at the unstable state $n = n_3 = 18.1$ an absolute value of $\tilde{A}_2(n) = A_2(n) = 1$.

$$2\frac{x-1}{\ln x} \leq x + 1 \qquad x > 0, \tag{35}$$

with $x = \gamma^+(n)/\gamma^-(n) > 0$.

The probability distribution then results in a competition between the coherent dynamics described by the drift motion and the diffusive motion which permits the system to leave states of local stability. In particular, a state that is favored in the presence of state-independent noise can become less favored in the presence of state-dependent noise (e.g., the noise amplitude might become considerably suppressed as a function of the state variable). Thus, correct relative stability is strongly impacted by the detailed noise variation along the escape route. We now evaluate the transition rates between the low-voltage state V_1 (left potential well in Figure 2) and the state of high voltage V_2 (right potential well in Figure 2), or vice versa.

• *Transition rates*

For a discrete process with nearest-neighbor transitions only, the mean first passage time $T(n_1, n_3)$ to get from the stable steady state $n = n_1$ to the unstable barrier top $n = n_3$ is explicitly given by [10]

$$T(n_1, n_3) \equiv T_+ = \Omega \int_{n_1}^{n_3} dy \frac{1}{\gamma^+(y) p_{St}(y)} \int_0^y dz p_{St}(z). \tag{36}$$

Because $p_{St}(n)$ is strongly peaked, we obtain, with a steepest descent approximation to Equation (36),

$$T_+ = \pi \frac{1}{\gamma^+(n_1)} \frac{1}{\sqrt{\phi_0''(n_1)|\phi_0''(n_3)|}} \exp\{\Omega[\phi_0(n_3) - \phi_0(n_1)]\}. \tag{37}$$

Because a random walker can at $n = n_3$ either proceed into the next well (i.e., $n = n_2$) or fall back toward $n = n_1$, the forward transition rate r^+ equals

$$r^+ = \frac{1}{2T_+} = \frac{1}{2\pi} \gamma^+(n_1) \sqrt{\phi_0''(n_1)|\phi_0''(n_3)|} \cdot \exp\{-\Omega[\phi_0(n_3) - \phi_0(n_1)]\}. \tag{38a}$$

Likewise, one finds for the high-voltage → low-voltage backward transition

$$r^- = \frac{1}{2T_-} = \frac{1}{2\pi} \gamma^+(n_2) \sqrt{\phi_0''(n_2)|\phi_0''(n_3)|} \cdot \exp\{-\Omega[\phi_0(n_3) - \phi_0(n_2)]\}, \tag{38b}$$

yielding for the slowest relaxation time λ_T, characteristic for the long-time dynamics in a bistable system, the value

$$\lambda_T = -(r^+ + r^-). \tag{39}$$

In terms of the Fokker–Planck approximation in Section 4, one finds from the corresponding mean first passage time expression [10, 12]

$$r^+_{KM} = \frac{1}{2\pi} \gamma^+(n_1) \sqrt{\psi_0''(n_1)|\psi_0''(n_3)|} \cdot \exp\{-\Omega[\psi_0(n_3) - \psi_0(n_1)]\}, \tag{40}$$

while the novel Fokker–Planck scheme in Section 5 yields

$$r^+_{NFP} = \frac{L(n_3)}{2\pi} \frac{\gamma^+(n_1)}{\gamma^+(n_3)} \sqrt{\phi_0''(n_1)|\phi_0''(n_3)|} \cdot \exp\{-\Omega[\phi_0(n_3) - \phi_0(n_1)]\}. \tag{41}$$

Because $\gamma^+(n_i) = \gamma^-(n_i)$, $i = 1, 2, 3$, one finds

$$L(n_i) = \tfrac{1}{2} A_2(n_i) = \tfrac{1}{2} \tilde{A}_2(n_i) = \gamma^+(n_i) = \gamma^-(n_i). \tag{42}$$

Thus, the new Fokker–Planck scheme gives rates that *coincide* precisely with Equations (38). Because the curvatures of ψ_0 and ϕ_0 do coincide, the prefactors of the two Fokker–Planck schemes coincide; the exponential leading parts, however, *differ in leading order.* The conventional Fokker–Planck modeling exponentially *overestimates* the transition rates; i.e.,

$$\frac{r^\pm_{KM}}{r^\pm} = \frac{r^\pm_{KM}}{r^\pm_{NFP}} = \exp(\Omega\Delta^\pm), \tag{43}$$

with

$$\Delta^\pm = -\int_{n_1}^{n_3} dy \left[\ln\frac{\gamma^+(y)}{\gamma^-(y)} - 2\frac{\gamma^+(y) - \gamma^-(y)}{\gamma^+(y) + \gamma^-(y)}\right] > 0 \tag{44}$$

being strictly positive. This intensive quantity characterizing the error in the transition-rate evaluation [see Equation (43)] is depicted in **Figure 5**.

6. Conclusions

In this paper we take a new look at the role of noise in negative differential resistance circuits. Due to a certain

mathematical inconvenience of modeling the noise dynamics with shot noise, i.e., with a master equation dynamics, one usually attempts a description in terms of a Fokker–Planck approximation. We have presented a novel Fokker–Planck scheme which possesses advantageous features over the conventional scheme of truncating the Kramers–Moyal expansion at the second order. The new Fokker–Planck modeling yields both the correct stationary probability and the deterministic law, and also correctly produces the transition rates, while with the conventional scheme one would exponentially overestimate these rates in leading order [see Equation (43) and Figure 5]. Physically this result has its origin in the systematic overestimation of the Kramers–Moyal diffusive noise strength, i.e, $A_2(n) > \tilde{A}_2(n)$; see below Equation (34). Thus the escape times are underestimated, yielding too-large escape rates. Moreover, it has been demonstrated elsewhere [9] that for processes possessing boundaries, the novel scheme preserves those boundaries. For example, if the state variable is strictly positive, the novel Fokker–Planck modeling yields a state-dependent diffusion coefficient that vanishes at the origin, and thus does not drive the system beyond its natural boundary toward negative state variables. The novel scheme has been constructed to accurately describe the long-time dynamics of the process, i.e., quantities such as the stationary probability and stationary correlations, etc. Nevertheless, both Fokker–Planck schemes of Sections 4 and 5 are approximations to the same master equation in the first place, and they certainly cannot reproduce all of the features of the master equation process. In particular, characteristic features that are sensitive at the order $1/\Omega$ clearly cannot be reproduced within a continuous state approximation.

While Rolf Landauer wrote his prescient paper on statistical densities and state-dependent noise in tunnel diodes over 25 years ago, it is interesting to note that research and development on small systems and on more sophisticated electronic devices with negative differential resistance continues to be an area of active and widespread interest today [13].

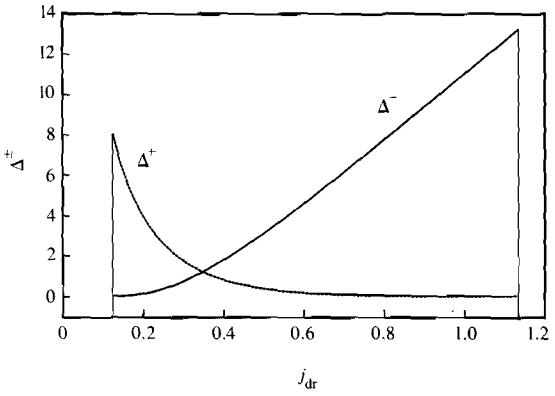

Figure 5

The quantities Δ^+ (broken line) and Δ^- (solid line) characterizing the error [see (43), (44)] for the forward transition rate r^+ and backward transition rate r^-, respectively, as a function of the driving current density $j_l \leq j_{dr} \leq j_u$.

References and notes

1. P. I. Kuznetsov, R. L. Stratonovich, and V. I. Tikhonov, "The Effect of Electrical Fluctuations on a Valve Oscillator," *Dokl. Akad. Nauk, SSSR* **97,** 639 (1954); R. L. Stratonovich, "Oscillator Synchronization in the Presence of Noise," *Radiotekhnika Electronica* **3,** 497 (1958); V. I. Tikhonov, "The Effect of Noise on the Operation of a Phase AFC Circuit," *Automatika Telemekhanika* **20,** 1188 (1959); see also the various other articles reprinted in *Nonlinear Transformation of Stochastic Processes*, P. I. Kuznetsov, R. L. Stratonovich, and V. I. Tikhonov, Eds., Pergamon Press, London, 1965.
2. R. Landauer, "Fluctuations in Bistable Tunnel Diode Circuits," *J. Appl. Phys.* **33,** 2209 (1962); a more recent summary of the basic points can be found in R. Landauer, "Stability in the Dissipative Steady State," *Phys. Today* **31,** 23 (1978).
3. P. Hänggi, A. R. Bulsara, and R. Junda, "Spectrum and Dynamic Response Function of Transmitted Light in the Absorptive Optical Bistability," *Phys. Rev. A* **22,** 671 (1980).
4. I. Matheson, D. F. Walls, and C. W. Gardiner, "Stochastic Models of First-Order Nonequilibrium Transitions in Chemical Reactions," *J. Stat. Phys.* **12,** 21 (1975); H. K. Jansen, "Stochastisches Reaktionsmodell für einen Nichtgleichgewichts-übergang," *Z. Phys.* **270,** 67 (1974); *Z. Phys. B* **20,** 338 (1975).
5. R. Lefever and W. Horsthemke, "Bistability in Fluctuating Environments: Implications in Tumor Immunology," *Bull. Math. Biol.* **41,** 469 (1979).
6. P. Hänggi and H. Thomas, "Stochastic Processes: Time Evolution, Symmetries and Linear Response" Section 6.3, "Bistable Tunnel Diode," *Phys. Rep.* **88,** 207 (1982).
7. N. G. van Kampen, "The Expansion of the Master Equation," *Adv. Chem. Phys.* **34,** 245 (1976).
8. P. Hänggi, "Nonlinear Fluctuations: The Problem of Deterministic Limit and Reconstruction of Stochastic Dynamics," *Phys. Rev. A* **25,** 1130 (1982).
9. H. Grabert, P. Hänggi, and I. Oppenheim, "Fluctuations in Reversible Chemical Reactions," *Physica* **117A,** 300 (1983).
10. P. Hänggi, H. Grabert, P. Talkner, and H. Thomas, "Bistable Systems: Master Equation Versus Fokker–Planck Modelling," *Phys. Rev. A* **29,** 371 (1984).
11. M. E. Daniel, "Development of Mathematical Models of Semiconductor Devices for Computer-Aided Circuit Analysis," *Proc. IEEE* **55,** 1913 (1967); H. Hamburger, P. Hänggi, and H. Thomas, "Stationäre Verteilung und Dynamisches Verhalten für ein Stochastisches Modell einer Bistabilen Tunneldiode," Diploma Thesis, University of Basel, Switzerland, 1976.
12. L. S. Pontryagin, A. A. Andronov, and A. Vitt, "On the Statistical Analysis of Dynamical Systems," *Zh. Eksper. Teor. Fiz.* **3,** 165 (1933).
13. See for example T. K. Woodward, T. C. McGill, and R. D. Burnham, "Realization of a Resonant Tunneling Transistor," *Appl. Phys. Lett.* **50,** 451 (1987).

Peter Hänggi *University of Augsburg, D-8900 Augsburg, Federal Republic of Germany.* Prof. Dr. Peter Hänggi received his Ph.D. in 1977 from the University of Basel, Switzerland. From 1977–1978 he was a postdoctoral Fellow at the University of Illinois at Urbana-Champaign, working on theoretical biophysics in the group of Prof. Frauenfelder. Then followed a year as a visiting professor at the University of Stuttgart, Federal Republic of Germany; in 1979 he worked as a postdoctoral Fellow at the University of California at San Diego. In 1980, he joined the faculty at the Polytechnic Institute of New York, first as Assistant Professor and then as tenured Associate Professor. Since June 1986, Dr. Hänggi has led the Theoretical Physics Department at the University of Augsburg. His research interests cover nonlinear dynamics, stochastic processes, random transport, and quantum-mechanical tunneling phenomena in the presence of dissipation. Dr. Hänggi is a member of the European, Swiss, German, and American physical societies.

Peter Jung *University of Augsburg, D-8900 Augsburg, Federal Republic of Germany.* Dr. Jung received his Diploma at the University of Ulm, Federal Republic of Germany, in 1983. From 1982–1985 he worked in the Department of Theoretical Physics in the group of Prof. H. Risken, and in 1985 received his Ph.D. from the University of Ulm. Since 1987 Dr. Jung has been an assistant in the group of Prof. P. Hänggi at the University of Augsburg, working in the field of stochastic processes and quantum optics.